

On possible types of magnetospheres of hot Jupiters

Zhilkin, A.G.*; Bisikalo D.V.

Institute of Astronomy of Russian Academy of Sciences, Moscow, Russia

ABSTRACT. We show that the orbits of exoplanets of the “hot Jupiter” type, as a rule, are located close to the Alfvén point of the stellar wind of the parent star. At this, many hot Jupiters can be located in the sub-Alfvén zone in which the magnetic pressure of the stellar wind exceeds its dynamic pressure. Therefore, magnetic field of the wind must play an extremely important role for the flow of the stellar wind around the atmospheres of the hot Jupiters. This factor must be considered both in theoretical models and in the interpretation of observational data. The analysis shows that many typical hot Jupiters should have shock-less intrinsic magnetospheres, which, apparently, do not have counterparts in the Solar System. Such magnetospheres are characterized, primarily, by the absence of the bow shock, while the magnetic barrier (ionopause) is formed by the induced currents in the upper layers of the ionosphere. We confirmed this inference by the three-dimensional numerical simulation of the flow of the parent star stellar wind around the hot Jupiter HD 209458b in which we took into account both proper magnetic field of the planet and magnetic field of the wind.

1 Introduction

When celestial bodies that have their own magnetic field interact with surrounding ionized matter, they create a cavity around themselves, which is named *magnetosphere*. In particular, such magnetospheres have Solar System planets blown over by the solar wind plasma [1]. The magnetosphere can have a complex structure and to change over the time, due to the heterogeneity and nonstationarity of the solar wind. Magnetic field of the planet prevents direct penetration of the solar wind plasma into the atmosphere. The boundary of the magnetosphere is a relatively thin current layer (*magnetopause*), which separates proper magnetic field of the planet from the magnetic field of the solar wind. Location of the magnetopause is determined by the balance of total pressure (the sum of the dynamic, gas, and magnetic pressure) from both sides of the boundary. However, in most cases, the total pressure from the outer side is equal to the dynamic pressure, while the pressure from the side of the planet is equal to the magnetic one. Such a situation exists, for instance, in the case of the Earth’s magnetosphere [2]. In the front of the magnetopause a *bow shock* forms, due to the supersonic flow regime. Between

*E-mail: zhilkin@inasan.ru

shock and magnetopause, a transition region exists, in which the plasma of the wind is heated, compressed, and retarded, changing the direction of the motion. An extended *magnetospheric tail* forms at the night side.

However, thousands of currently known exoplanets must have magnetospheres too. Magnetospheres of the exoplanets may have their own specific features. In the present paper, we will focus on the structure of the magnetospheres of the hot Jupiters. “Hot Jupiters” are exoplanets with the mass comparable to the mass of Jupiter, located in the immediate vicinity of the parent star [3]. The first hot Jupiter was discovered in 1995 [4]. Because of the proximity of the planets to the parent stars and their relatively large size, gas envelopes of the hot Jupiters can overflow their Roche lobes, leading to the formation of the outflows from the vicinities of the Lagrange points L_1 and L_2 [5,6]. This is indirectly indicated by excessive absorption in the near-UV range, observed for some planets [7–12]. These conclusions are confirmed theoretically by the one-dimensional aeronomic models [3, 13–16].

Based on the three-dimensional numerical modeling, it was shown in the series of studies [17–23] that, depending on the parameters of a hot Jupiter, gas envelopes of three main types can form [18]. To the first type belong *closed envelopes*, in which planet atmosphere resides inside its Roche lobe. Into the second type fit *open envelopes* that are formed by the outflows from the nearest Lagrange points. Finally, one can distinguish *quasi-closed envelopes* of an intermediate type, for which stellar wind dynamic pressure stops the outflow outside the Roche lobe. Calculations have shown that in the cases of closed and quasi-closed envelopes the rate of mass loss by hot Jupiters is significantly lower, compared to the case of open envelopes. Arakcheev et al. [24] presented results of numerical modeling of the flow structure in the vicinity of the hot Jupiter WASP 12b that took into account the influence of the planet’s magnetic field. It was shown that the presence of even a relatively weak planet’s magnetic field (the magnetic moment comprised 10 per cent of Jupiter’s magnetic moment) may lead to a noticeable decrease of the rate of mass loss, compared to the net gas-dynamical case. In addition, magnetic field may cause fluctuations in the outer parts of the envelope [25].

There is an unaccounted factor in the studies quoted above, related to the magnetic field of the stellar wind. However, the analysis performed in the present paper showed that it is very important. The fact is that, apparently, many hot Jupiters are located in the sub-Alfvén zone of the stellar wind, where the magnetic pressure exceeds the dynamic one. Therefore, accounting for magnetic field of the wind, formally, switches the flow of the wind around a hot Jupiter from supersonic regime to subsonic one. As a result, in this mode, bow shock should not form in the front of the atmosphere [26], i.e., the flow is shock-less. This conclusion follows from the assumption that the magnetic field of the wind is determined by the average magnetic field at the surface of the Sun, which is about 1 G. However, magnetic fields of solar type stars can range from about 0.1 to several G [27, 28]. In addition, hot Jupiters can have parent stars not of solar type only, because their spectral types are from F to M. The azimuthal component of the magnetic field of the stellar wind is determined by the angular velocity of the stellar spin, which, in turn, also depends on the spectral type [28]. If all these additional factors are taken into account, it appears that some hot Jupiters may be located not only in the transition region, separating the sub-Alfvén and super-Alfvén zones, but to move even into the super-Alfvén zone. This circumstance considerably expands the set of possible

configurations of the magnetospheres of hot Jupiters.

It should be noted that there is a simple way to approximate account of magnetic wind field in the net gas-dynamical calculations. To do this, instead of gas pressure P , one needs to use full pressure $P_T = P + B^2/(8\pi)$. It is not difficult to see that this is equivalent to the replacement of the temperature T of the wind by the temperature

$$\tilde{T} = T \left(1 + \frac{u_A^2}{2c_T^2} \right), \quad (1)$$

where c_T is the isothermal sound velocity, u_A is the Alfvén velocity. In this case, the spatial distribution of the magnetic field B and, consequently, of the temperature \tilde{T} should be determined by some kind of magnetohydrodynamical wind model. Such an amendment can effectively increase the wind temperature and to switch the flow around the planet into subsonic mode.

In the present paper, we analyzed the possible types of magnetospheres of hot Jupiters, taking into account possible outflows resulting from Roche lobe overflow. The results of numerical simulations using three-dimensional magnetohydrodynamical model confirm the conclusions obtained on the basis of simple theoretical considerations.

The structure of the article is as follows. In §2 we describe the model of magnetic field of the stellar wind applied by us. In §3 we analyze possible types of magnetospheres of hot Jupiters. In §4 numerical model is described. In §5 results of calculations are presented. The summary of the main results of the study follows in §6.

2 The model of magnetic field of the stellar wind

In our numerical model, we will rely on the well-studied properties of the solar wind. As it is shown by numerous ground- and space-based studies (see, for instance, the recent review [29]), magnetic field of the solar wind has a rather complex structure. Schematically, this structure is shown in Fig. 1. In the corona region, magnetic field is essentially non-radial, because there it is mainly defined by the own magnetic field of the Sun. At the border of the corona, at the distance of several solar radii, the field, to a large accuracy, becomes completely radial. Farther, *heliospheric region* is located, in which the magnetic field to a substantial extent is determined by the properties of the solar wind. In the heliosphere, with the distance from the center, magnetic field lines gradually twist into a spiral due to the rotation of the Sun and therefore (especially at large distances) the magnetic wind field can be described with a good accuracy using the simple Parker model [30].

However, the observed magnetic field in the solar wind is not axisymmetric and has a pronounced sector structure. This is due to the fact that in the different points of the spherical surface of the corona the field may have different polarity (direction of the magnetic field lines relative to the direction of the normal vector), for example, due to the inclination of the solar magnetic axis to the axis of its rotation. As a result, in the ecliptic plane, in the solar wind form two clearly distinguished sectors with different magnetic field directions. In one sector, magnetic field lines are directed to the Sun, while in the opposite sector they are directed from the Sun. These two sectors are separated by *heliospheric current sheet*, which is shown in Fig. 1 in gray. To the current sheet itself

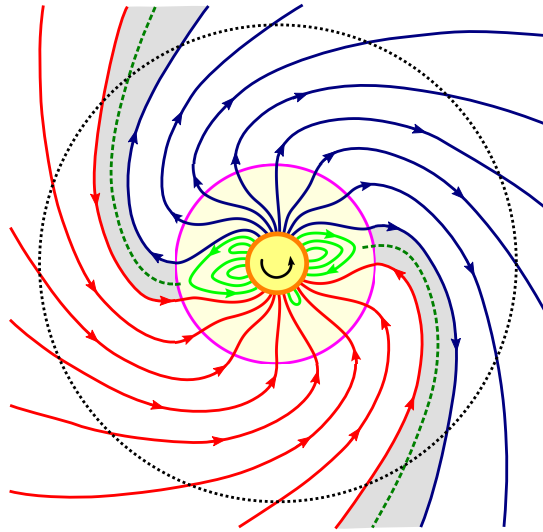


Fig. 1. Schematic picture of the solar wind in the ecliptic plane. Small dyed circle in the center corresponds to the Sun. The arrow shows the direction of rotation of the Sun. The boundary of the middle circle defines the corona region, at the border of which magnetic field becomes completely radial. The shaded gray areas correspond to the zones of the heliospheric current sheet which is shown by dashed lines running from the corona to the periphery. It separates magnetic field of the solar wind with different directions of magnetic field lines (from the Sun or to the Sun). The orbit of the planet (shown by a dotted circle) is located in the heliospheric region. (A color version of the Figure is available in the electronic version of the journal.

correspond to two twisted dashed lines going from the border of the corona to the periphery of the heliosphere. The heliospheric current sheet rotates with the Sun and, therefore, the Earth, as it moves around the Sun, crosses it many times a year (about 13 times), moving from the solar wind sector with one polarity of the magnetic field into the adjacent sector with opposite polarity of the field.

In this paper we do not take into account possible sectoral structure of the wind magnetic field, focusing on the impact of its global parameters. More detailed consideration and account of the unquestionably important effects associated with the transition of the planets through the current sheet and the polarity reversal of the magnetic field, we plan to carry out in the further studies. On the top of everything else, in our model we will assume that the orbit of a hot Jupiter is located in the heliospheric region beyond the border of the corona. In Fig. 1 the orbit of the planet is shown as a large dotted circle.

To the first approximation, to describe the magnetic field \mathbf{B} of the wind in the heliospheric region, one can use the simple axisymmetric model described by Baranov and Krasnobayev in the monograph [31]. In the inertial reference frame in the spherical coordinates (r, θ, φ) magnetic field and stellar wind velocity can be represented as follows:

$$\mathbf{B} = B_r(r)\mathbf{n}_r + B_\varphi(r, \theta)\mathbf{n}_\varphi, \quad \mathbf{v} = v_r\mathbf{n}_r + v_\varphi(r, \theta)\mathbf{n}_\varphi. \quad (2)$$

At difference to [31], in these expressions we took into account the dependence of B_φ and v_φ on the angle θ , since our model is three-dimensional. More, for simplicity, in the vicinity of the planet we will consider the radial component of velocity as constant and equal to v_w .

In such an approximation, the structure of stellar wind is described by a system of equations containing equation of continuity

$$\frac{1}{r^2} \frac{\partial}{\partial r} (r^2 \rho v_r) = 0, \quad (3)$$

Maxwell equation ($\nabla \cdot \mathbf{B} = 0$)

$$\frac{1}{r^2} \frac{\partial}{\partial r} (r^2 B_r) = 0, \quad (4)$$

equation for angular momentum

$$\frac{\rho v_r}{r} \frac{\partial}{\partial r} (r v_\varphi) = \frac{B_r}{4\pi r} \frac{\partial}{\partial r} (r B_\varphi) \quad (5)$$

and equation of induction

$$\frac{1}{r} \frac{\partial}{\partial r} (r v_r B_\varphi - r v_\varphi B_r) = 0. \quad (6)$$

From the equation of continuity (3) we find

$$\rho = \rho_w \left(\frac{A}{r} \right)^2, \quad (7)$$

where A is the large semiaxis of the orbit of the planet, ρ_w — the density of the stellar wind at the orbit of the planet. From the Maxwell equation (4) we obtain

$$B_r = B_0 \left(\frac{R_s}{r} \right)^2 = B_w \left(\frac{A}{r} \right)^2, \quad (8)$$

where R_s is the radius of the star, B_0 — field strength at the stellar surface, B_w — radial component of the field at the orbit of the planet.

Let note that from the Eqs. (2) and (3) it follows

$$\frac{B_r}{4\pi\rho v_r} = \frac{r^2 B_r}{4\pi r^2 \rho v_r} = \text{const.} \quad (9)$$

This circumstance allows to obtain from the Eqs. (4) and (5) two integrals of motion:

$$r v_\varphi - \frac{B_r}{4\pi\rho v_r} r B_\varphi = L(\theta), \quad (10)$$

$$r v_r B_\varphi - r v_\varphi B_r = F(\theta). \quad (11)$$

The function $F(\theta)$ may be found from the boundary conditions at the stellar surface ($r = R_s$):

$$B_\varphi = 0, \quad B_r = B_0, \quad v_\varphi = \Omega_s R_s \sin \theta, \quad (12)$$

where Ω_s is angular velocity of the stellar spin. Therefore,

$$F(\theta) = -\Omega_s R_s^2 \sin \theta B_0 = -\Omega_s r^2 \sin \theta B_r. \quad (13)$$

Taking into account the latter expression, solutions of Eqs. (4) and (5) may be written as:

$$v_\varphi = \frac{\Omega_s \sin \theta r - \lambda^2 L(\theta)/r}{1 - \lambda^2}, \quad (14)$$

$$B_\varphi = \frac{B_r}{v_r} \lambda^2 \frac{\Omega_s \sin \theta r - L(\theta)/r}{1 - \lambda^2}. \quad (15)$$

Here, λ is Alfvén Mach number for the radial components of the velocity and magnetic field,

$$\lambda^2 = \frac{4\pi\rho v_r^2}{B_r^2}. \quad (16)$$

Close to the stellar surface, the radial wind velocity v_r should be lower than the Alfvén velocity $u_A = |B_r|/\sqrt{4\pi\rho}$ and the parameter $\lambda < 1$. At large distances, the radial velocity v_r , on the contrary, exceeds Alfvén velocity u_A ($\lambda > 1$). This means that at certain distance from the center of the star $r = a$ (Alfvén point) the parameter $\lambda=1$. The domain $r < a$ can be called *sub-Alfvén* zone of the stellar wind, and the region $r > a$ — *super-Alfvén* zone, respectively.

The values v_φ and B_φ in the expressions (14) and (15) should be continuous in the Alfvén point $r = a$. Therefore, it is necessary to set

$$L(\theta) = \Omega_s \sin \theta a^2. \quad (17)$$

As a result, we find the final solution

$$v_\varphi = \Omega_s \sin \theta r \frac{1 - \lambda^2 a^2/r^2}{1 - \lambda^2}, \quad (18)$$

$$B_\varphi = \frac{B_r}{v_r} \Omega_s \sin \theta r \lambda^2 \frac{1 - a^2/r^2}{1 - \lambda^2}. \quad (19)$$

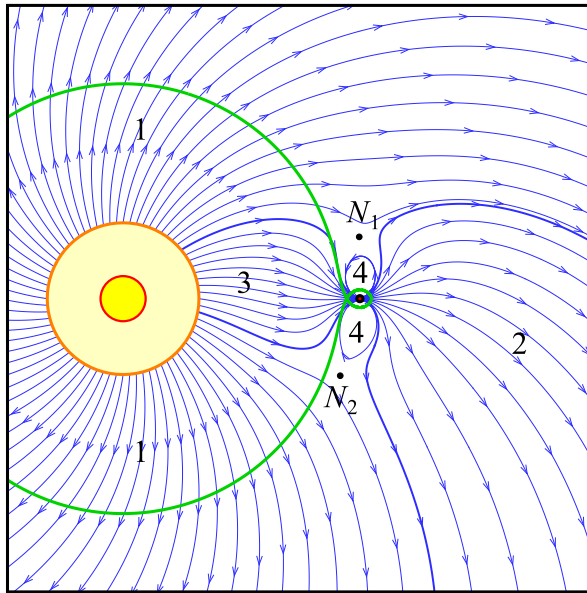


Fig. 2. Initial distribution of the magnetic field in the equatorial plane for the case $B_0 = 10^{-3}$ G. Thick solid line shows the Roche lobe. The star is indicated by a color ring, the inner radius of which corresponds to the radius of the star and the outer radius — to the radius of the corona. The numbers in the diagram label four magnetic zones. Neutral points are marked as N_1 and N_2 . (A color version of the Figure is available in the electronic version of the journal.)

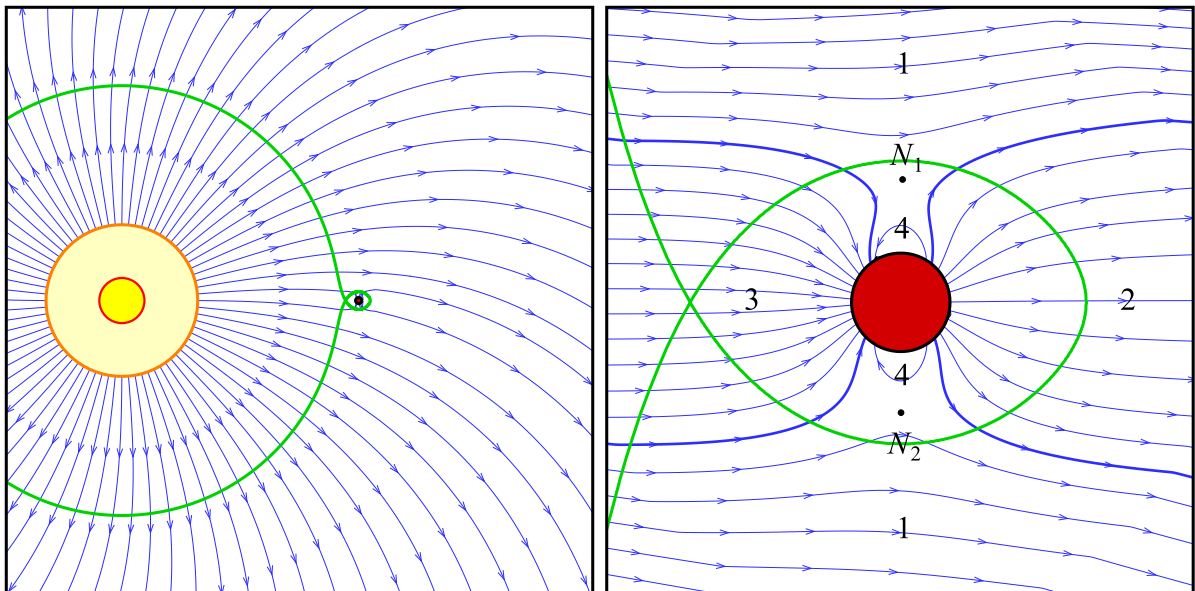


Fig. 3. Initial distribution of the magnetic field in the equatorial plane for the case $B_0 = 1$ G. Vicinity of the planet is shown in the blown-up image to the right. Notation as in Fig. 2.

We use these relations in the numerical model to describe the stellar wind.

In Figs. 2 and 3 we show initial (without the outflows from the envelope) structure of the magnetic field in the vicinity of the hot Jupiter HD 209458b, for which we carried out numerical modeling in this paper. The parameters of the magnetic field (the strength of the field and the orientation of the magnetic axis) of the planet correspond to those set in the calculations (see §5). In Fig. 2 we show the distribution of magnetic field lines for the case $B_0 = 10^{-3}$ G, which corresponds to the weak wind field. The star is to the left and the planet is to the right. The star is indicated by a color ring. The inner radius of the ring corresponds to the stellar surface, while the outer radius — to the surface of the corona. The radius of the corona is about three times larger than the radius of the star. Thick solid line labels the boundary of the Roche lobe. Magnetic field lines are shown by solid lines with arrows. It is easy to see that the magnetic field can be clearly divided into four magnetic zones, which are labeled by the corresponding numbers. Zone 1 is characterized by the open stellar magnetic lines; magnetic lines originate at the surface of the star and extend to infinity. Zone 2 is defined by the similar open magnetic field lines of the planet. In zone 3, magnetic lines are common to the star and the planet, they originate at the surface of the star and terminate at the surface of the planet. Finally, zone 4 consists of the closed lines of the planet field. At neutral points the direction of the magnetic field is undefined. In the equatorial plane, these points are labeled as N_1 and N_2 . In the space, the set of these points forms a neutral line similar to a circle, with the shape determined by the orientation of the magnetic axis of the planet.

In Fig. 3 we show the distribution of the magnetic field lines for the case $B_0 = 1$ G, which corresponds to a strong wind field. Like in the previous case, one can also distinguish all four magnetic zones and to define position of the neutral points (see the right panel of the Figure). It should be noted, that such a situation is not at all exotic, since such a field strength must be typical for the stars of this type (spectral type of HD 209458 is G0 V). For instance, it is well known that the average magnetic field at the surface of the Sun (including spots) is, approximately, 1 G.

3 Magnetospheres of the hot Jupiters

Under assumption of a constant radial velocity of the stellar wind $v_r = v_w$, it is possible to derive a simple expression for the Alfvén Mach number:

$$\lambda^2 = \frac{4\pi\rho_w v_w^2}{B_w^2} \left(\frac{r}{A}\right)^4 = \lambda_w^2 \left(\frac{r}{A}\right)^4, \quad (20)$$

where

$$\lambda_w = \frac{\sqrt{4\pi\rho_w} v_w}{B_w} \quad (21)$$

defines the value of λ at the orbit of the planet. At this, Alfvén point is defined by the expression

$$a = \frac{A}{\sqrt{\lambda_w}}. \quad (22)$$

In the solar wind, Alfvén radius is [31]

$$a = 0.1 \text{ AU} = 22R_\odot. \quad (23)$$

Since the semi-major axis of the orbit of the innermost planet, Mercury, is $0.38 \text{ AU} = 82R_\odot$, this means that all planets of the Solar System are located in the super-Alfvén zone of the solar wind. In the solar wind, the sonic point, where the wind velocity becomes equal to the sound velocity, is even closer to the Sun, at the distance of approximately $0.05 \text{ AU} = 11R_\odot$. Then the magnetospheres (if any) of all planets in the Solar System have a similar structure, resembling that of the Earth magnetosphere. They are characterized by the following set of the basic elements: bow shock, transition region, magnetopause, radiation belts, magnetospheric tail.

In the case of hot Jupiters, because of their proximity to the parent star, the structure of the magnetosphere may be completely different. Let consider as an example two typical hot Jupiters HD 209458b and WASP 12b. For the first planet one has: $A = 10.2R_\odot$, $B_w = 0.0125 \text{ G}$, $\lambda_w = 0.37$, $a = 16.8R_\odot$. At this, at the orbit of the planet the ratio $B_\varphi/B_r = 0.12$. For another planet $A = 4.9R_\odot$, $B_w = 0.1 \text{ G}$, $\lambda_w = 0.045$, $a = 23.2R_\odot$ and the ratio of the azimuthal field and the radial one at the orbit of the planet is $B_\varphi/B_r = 0.01$. Thus, these hot Jupiters are located in the sub-Alfvén zone of the stellar wind. Accounting for the orbital motion may partially change the situation. In fact, the full wind velocity relative to the planet in this case will be equal to $v = \sqrt{v_r^2 + v_\varphi^2}$, where $v_\varphi = \Omega A$, $\Omega = \sqrt{GM/A^3}$ is the orbital angular velocity of the planet, G is gravity constant, $M = M_p + M_s$ — the total mass of the system, M_p — the mass of the planet, M_s — the mass of the star. Substituting the values of the corresponding parameters at the orbits, we find the ratio $v/u_A = 0.65$ for the planet HD 209458b and $v/u_A = 0.11$ for the planet WASP 12b. As it can be seen, in the first case, the value of the total wind velocity turns out to be quite close to the Alfvén velocity. Therefore, it is possible to consider that the planet HD 209458b is located in the border region between sub-Alfvén and super-Alfvén zones of the wind, since even small magnetic field fluctuations (within a factor of 1.5 to 2) will be sufficient to change the mode of the wind flow around the planet.

Because for these hot Jupiters Alfvén Mach number $\lambda = v_r/u_A$ turns out to be less than 1, the ratio v_r/u_F , where $u_F = \sqrt{c_s^2 + u_A^2}$ and c_s — the sound velocity, will also be less than 1, since it is obvious that $u_F > u_A$ and, therefore, the ratio $v_r/u_F < v_r/u_A$. In other words, in the neighborhood of a hot Jupiter, stellar wind velocity will be lower than the fast magneto-sonic velocity. In usual gas dynamics this case corresponds to the subsonic flow around a body, in which the bow shock does not form. Thus, we arrive to the following conclusion: the flow of stellar wind around such a hot Jupiter should be *shock-less*. In the structure of the magnetosphere of the hot Jupiter bow shock should be absent.

This conclusion is based on the analysis of the parameters of two typical hot Jupiters, HD 209458b and WASP 12b. However, apparently, it will remain valid for many other exoplanets of this type. To verify this statement, we processed the relevant data for a sample of 210 hot Jupiters taken from the database at www.exoplanet.eu. The sampling was carried out by the masses of the planets (mass of the planet $M_p > 0.5M_{\text{jup}}$, where M_{jup} is the mass of Jupiter), the orbital periods ($P_{\text{orb}} < 10 \text{ day}$) and the semi-major orbits ($A < 10R_\odot$). In addition, only those planets were kept for which all necessary data are known.

As a model of the stellar wind in the immediate vicinity of the Sun at the distances $1R_\odot < r < 10R_\odot$ we used results of the calculations from [32]. According to the obtained

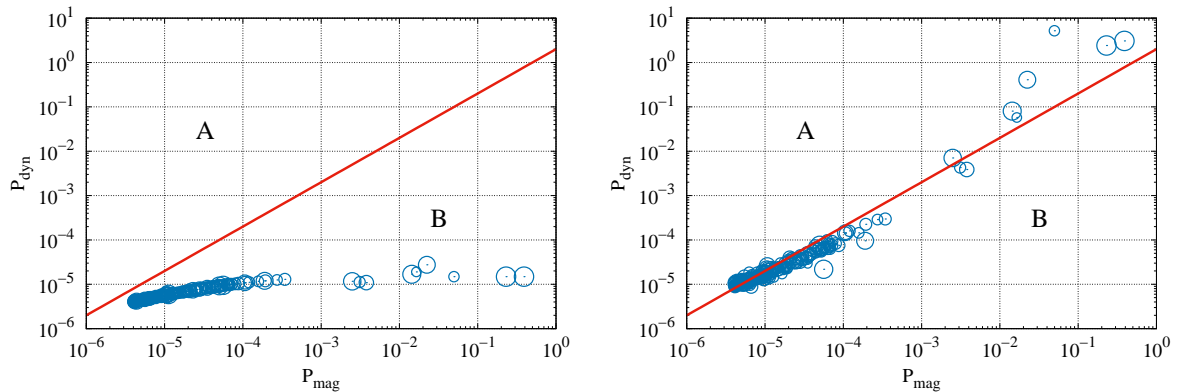


Fig. 4. Distribution of hot Jupiters in the two-dimensional diagram $P_{\text{mag}} - P_{\text{dyn}}$ (see the text for details). For the data in the left panel, Alfvén Mach numbers were calculated taking into account only wind velocity. In the right panel computed data take into account orbital velocities of the planets. The parameters of the planets are taken from the database at www.exoplanet.eu. The data for 210 hot Jupiters was used. To positions of the planets correspond the centers of the circles. The size of the circles corresponds to the masses of the planets (in the logarithmic scale). Solid line shows position of the Alfvén point. The letters label super-Alfvén zone (A) and sub-Alfvén zone (B). (A color version of the Figure is available in the electronic version of the journal).

profiles of density $\rho(r)$ and radial velocity $v_r(r)$, for every hot Jupiter from the sample we calculated the dynamic pressure of the wind at the orbit of the planet

$$P_{\text{dyn}} = \rho(A) \left[v_r^2(A) + \frac{G(M_s + M_p)}{A} \right] \quad (24)$$

and magnetic pressure

$$P_{\text{mag}} = \frac{B_r^2(A)}{8\pi}, \quad (25)$$

where the value of the radial field was calculated by the formula $B_r(A) = B_0(R_\odot/A)^2$ with the parameter $B_0 = 1$ G. The resulting distribution of hot Jupiters in the two-dimensional diagram $P_{\text{mag}} - P_{\text{dyn}}$ is presented in Fig. 4. The left panel of the Figure presents results of computations in which in calculation of the Alfvén Mach number only radial wind velocity was taken into account. The right panel presents distribution of planets for the case when their orbital velocity was taken into account. To the positions of the planets correspond the centers of the circles; the sizes of the latter are determined by their mass M_p in the logarithmic scale. The solid line shows position of the Alfvén point, to which corresponds a simple ratio $P_{\text{dyn}} = 2P_{\text{mag}}$.

As it is seen from the resulting distribution, many hot Jupiters from this sample reside in the sub-Alfvén zone of the stellar wind. An account for the orbital velocity substantially shifts the entire sequence upward in the diagram, into direction of the super-Alfvén wind zone. Note that most of the planets in this diagram form a certain regular sequence (see lower left corner of the diagram). These planets are located quite far from the stars, where the dependencies of density and wind velocity on the radius are well described by power laws. Planets close to the stars are scattered over diagram in a rather chaotic

manner. For these planets, the magnitude of the dynamic wind pressure is determined mainly by their orbital velocity. Note that the orbital velocity of the planet depends not on the radius of the orbit only, but also (albeit to a rather small extent) on the mass of the planet.

It should be borne in mind that this distribution was obtained for the solar wind in the model of a quiet Sun. At this, we assumed that the average value of the magnetic field at the surface of the Sun is 1 G. Even for the Sun, during its activity cycle, positions of the hot Jupiters in the diagram in Fig. 4 may change in any direction with respect to the Alfvén point. In reality, every planet of our sample is flown around not by the solar wind, but by the stellar wind of the parent star. The parameters of this wind can significantly differ from the solar wind ones. This means that the flow of the stellar wind around the atmosphere of the planet must be investigated separately in each particular case, taking into account the individual characteristics of the planet and the parent star. In particular, in our numerical model, we can vary the value of the average field B_0 at the surface of the star (i.e., at $r = R_s$, and not at the surface of the Sun at $r = R_\odot$). The strength of the average magnetic field of the solar type stars can range from about 0.1 G to about 5 G [27]. In addition, the radii of the stars can be both smaller and larger than the solar one. For example, the radius of the star WASP 12 is $1.57 R_\odot$. Therefore, if one would take the corresponding value of the average field $B_0 = 1$ G, magnetic induction in the vicinity of the planet WASP 12b will be, approximately, by factor 2.5 larger than the magnetic induction of the solar wind at the same distance from the Sun. Using the same simple method it is possible to model numerically formation of magnetospheres of hot Jupiters of all major types.

Let characterize the magnetosphere by three characteristic parameters: dimensions of *ionospheric envelope* R_{env} , magnetopause radius R_{mp} , and the radius of the bow shock R_{sw} . As the ionospheric envelope, we mean the upper layers of the atmosphere of a hot Jupiter, which consist of almost completely ionized gas [22]. In our terminology, closed ionospheric envelope corresponds to the case when the atmosphere of a hot Jupiter is entirely located within its Roche lobe. Open ionospheric envelope corresponds to the case when a hot Jupiter overflows its Roche lobe. The overflow results in planetary outflows from the vicinities of the Lagrange points L_1 and L_2 . For the magnetopause and shock wave, one can take the distances from the center of the planet to the corresponding frontal collision point. Depending on the relationship between these parameters, we can suggest the following simple classification of the possible types of the magnetospheres of hot Jupiters.

Type A. The parameter $\lambda_w > 1$, therefore, a bow shock settles in the front of the magnetosphere, $R_{\text{sw}} < \infty$. Taking into account relations between the remaining parameters we obtain two special cases.

Subtype A1 (intrinsic magnetosphere with bow shock): $R_{\text{env}} < R_{\text{mp}}$. In this case, magnetic field of the planet is rather strong, therefore, the magnetopause is located outside the ionospheric envelope. Corresponding scheme of the structure of such a magnetosphere for the cases of closed and open ionospheric envelopes is shown in Fig. 5. In the solar system, similar situation for a closed ionospheric envelope corresponds, for instance, to the magnetospheres of the Earth and Jupiter.

Subtype A2 (induced magnetosphere with bow shock): $R_{\text{env}} > R_{\text{mp}}$. In this case, magnetic field of the planet is weak and, therefore, the magnetopause is located inside

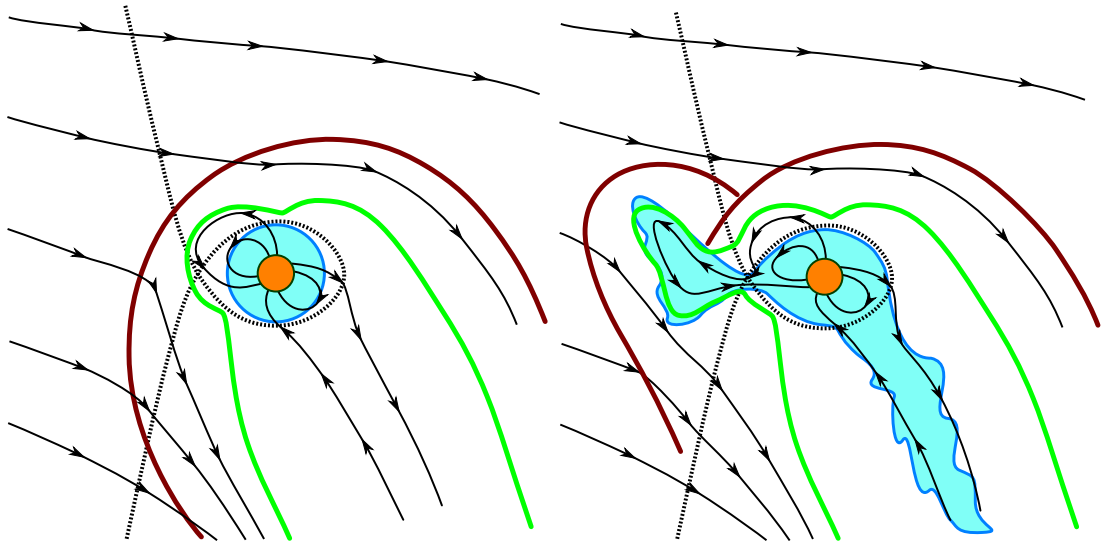


Fig. 5. Schematic representation of the structure of the *A1*-subtype magnetosphere in the case of a closed (left) and open (right) ionospheric envelope of a hot Jupiter. The lines with arrows correspond to the magnetic field lines. Dotted line shows the border of the Roche lobe. The hatched area corresponds to the gas envelope of the planet. Positions of the shock wave (outer solid line) and magnetopause (inner solid line) are shown. (A color version of the Figure is available in the electronic version of the journal).

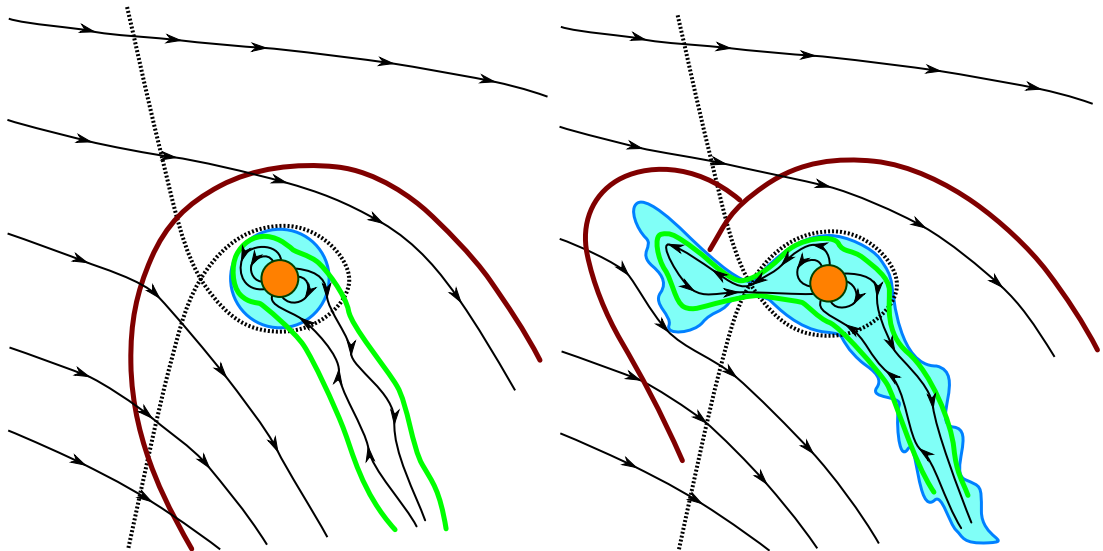


Fig. 6. Schematic representation of the structure of *A2*-subtype magnetosphere of in the the case of a closed (left) and open (right) ionospheric envelope of a hot Jupiter. Notation as in Fig. 5. (A color version of the Figure is available in the electronic version of the journal.)

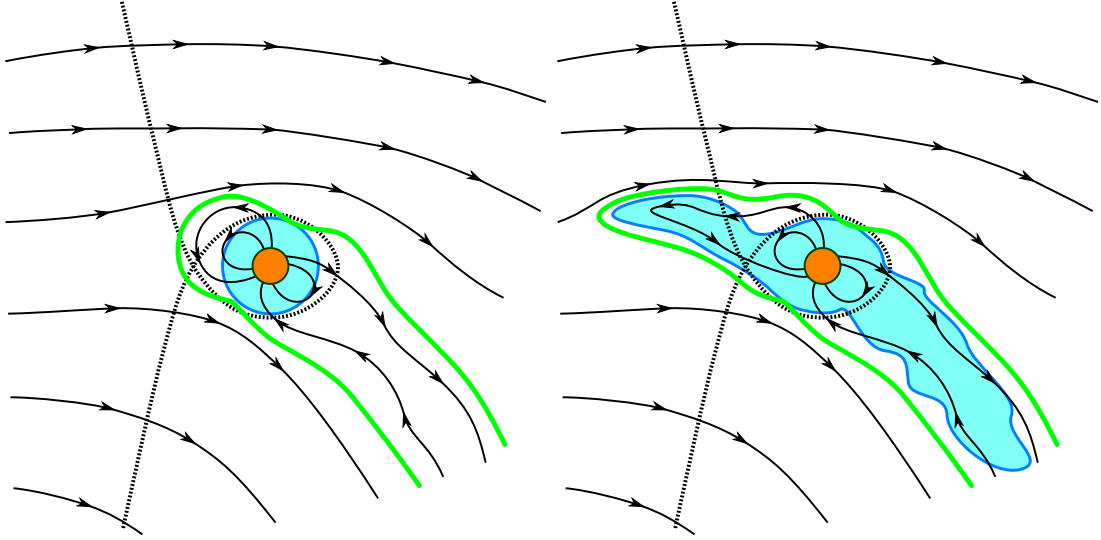


Fig. 7. Schematic representation of the structure of $B1$ -subtype magnetosphere in the case of a closed (left) and open (right) ionospheric envelope of a hot Jupiter. Notation as in Fig. 5. (A color version of the Figure is available in the electronic version of the journal.)

the ionospheric envelope. Schematically, the structure of such a magnetosphere for the cases of closed and open ionospheric envelopes is shown in Fig. 6. In the Solar System, this situation for the case of a closed ionospheric envelope corresponds to the Venus magnetosphere (and, to some extent, to the Mars one).

Induced magnetosphere [33] is formed by the currents that are excited in the upper layers of the ionosphere. Excitation mechanism of these currents is associated with the phenomenon of unipolar induction [34], arising when the conductor moves perpendicularly to the magnetic field. The currents induced in the ionosphere partially shield the magnetic field of the wind. As a result, magnetic lines of the arising field enshroud the ionosphere of the planet, forming a peculiar magnetic barrier (*ionopause*). Bow shock sets directly in the front of this barrier. On the night side, a magnetospheric tail is formed, which can be partially filled by plasma from the ionosphere. Unlike the proper magnetosphere, the orientation of the magnetic field in the induced magnetosphere is completely determined by the wind field. As a result, entire structure of the magnetosphere will track the direction to the star as the planet moves along its orbit.

Type **B**. The parameter $\lambda_w < 1$ and the bow shock does not form. Therefore, we can formally assume that $R_{sw} = \infty$. Again, two particular cases can be distinguished.

Subtype $B1$ (*shock-less intrinsic magnetosphere*): $R_{env} < R_{mp}$. This situation arises in the case of a sufficiently strong own magnetic field of the planet. As a result, the boundary of the magnetopause will be located outside the ionospheric envelope. The structure of the magnetosphere of this type for the cases of closed and open ionospheric envelopes are shown in Fig. 7. It should be noted that, apparently, this case is rather exotic, because the own magnetic field of a hot Jupiter must be relatively weak.

Subtype $B2$ (*Shock-less induced magnetosphere*): $R_{env} > R_{mp}$. It is possible that for the hot Jupiters this is the most common situation. In this case, the magnetopause is formally located inside the ionospheric envelope. Therefore, the outflows from the

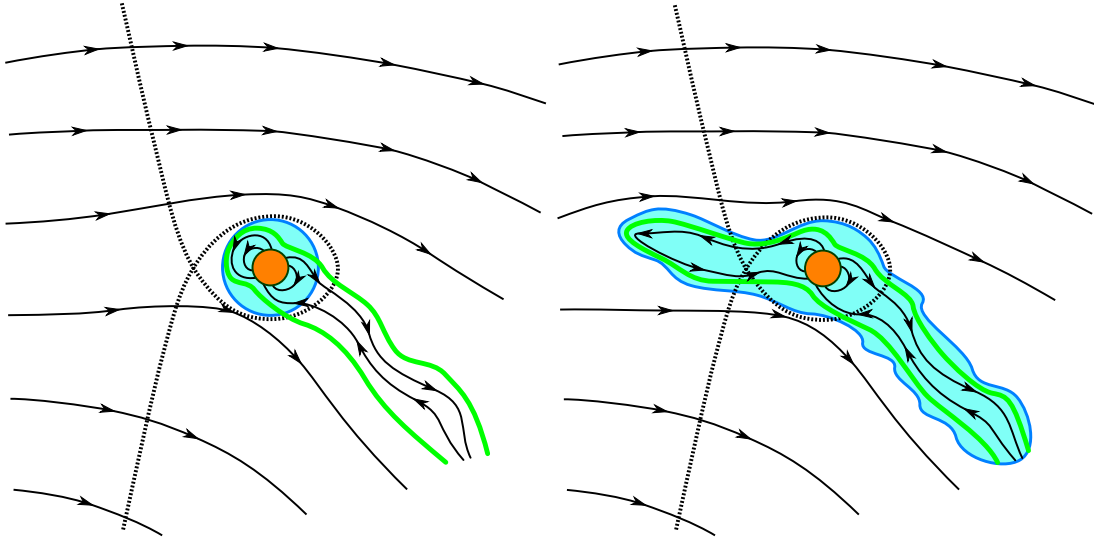


Fig. 8. Schematic representation of the structure of $B2$ -subtype magnetosphere in the case of a closed (left) and open (right) ionospheric envelope of a hot Jupiter. Notation as in Fig. 5. (A color version of the Figure is available in the electronic version of the journal.)

envelope interact directly with the magnetic field of the stellar wind. The structure of the magnetosphere of this type for the cases of closed and open ionospheric envelopes is shown in Fig. 8. Taking into account possible types of gas envelopes of hot Jupiters [18], it is possible to distinguish here additional subtypes, corresponding, for instance, to closed, quasi-closed, and open envelopes..

Type C. Parameter $\lambda_w \approx 1$. This is an intermediate type of magnetospheres corresponding to the “gray” zone. In particular, in this case the planet itself can be located in the sub- or super-Alfvén wind zone at the time, when outflowing ionospheric envelope, due to its rather large extent, may intersect the Alfvén point and partially flow into the opposite wind zone. Such an unusual situation may appear fairly common for hot Jupiters, since their orbits are usually located close to the Alfvén point (see the distribution of hot Jupiters in the diagram in Fig. 4). This case must be investigated separately.

4 Description of the model

4.1 Basic equations

To describe the structure of the flow in the vicinity of hot Jupiter, we will use the system of equations of ideal one-fluid magnetic hydrodynamics with background field [24,35,36]. Under this approach, the full magnetic field \mathbf{B} is represented as a superposition of the background magnetic field \mathbf{H} and the magnetic field \mathbf{b} induced by the currents in the plasma itself, $\mathbf{B} = \mathbf{H} + \mathbf{b}$. Since the background field in the problem in question is generated by the sources outside the computational domain, in the the computational domain it must satisfy the potential condition, $\nabla \times \mathbf{H} = 0$. Just this external field property is used for its partial exclusion from the equations of magnetic hydrodynamics

[37, 38]. In addition, in our model we assume that the background magnetic field is steady, $\partial \mathbf{H} / \partial t = 0$. This corresponds to the case, when the spin of a hot Jupiter's is synchronized with its orbital motion.

Bearing in mind condition $\nabla \times \mathbf{H} = 0$, equations of ideal magnetohydrodynamics may be written as

$$\frac{\partial \rho}{\partial t} + \nabla \cdot (\rho \mathbf{v}) = 0, \quad (26)$$

$$\rho \left[\frac{\partial \mathbf{v}}{\partial t} + \mathbf{v} \cdot \nabla \mathbf{v} \right] = -\nabla P - \mathbf{b} \times \nabla \times \mathbf{b} - \mathbf{H} \times \nabla \times \mathbf{b} - \rho \mathbf{f}, \quad (27)$$

$$\frac{\partial \mathbf{b}}{\partial t} = \nabla \times (\mathbf{v} \times \mathbf{b} + \mathbf{v} \times \mathbf{H}), \quad (28)$$

$$\rho \left[\frac{\partial \varepsilon}{\partial t} + \mathbf{v} \cdot \nabla \varepsilon \right] + P \nabla \cdot \mathbf{v} = 0. \quad (29)$$

Here ρ is density, \mathbf{v} — velocity, P — pressure, ε — specific internal energy. For convenience of numerical modeling, in these equations the system of units without factor 4π is used. It is assumed that the matter may be considered as an ideal gas with an equation of state

$$P = (\gamma - 1)\rho\varepsilon, \quad (30)$$

where $\gamma = 5/3$ — adiabatic exponent.

Computations were carried out in a rotating reference frame, in which the positions of the centers of star and planet did not change. In this case, the angular velocity vector of rotation of the reference frame $\boldsymbol{\Omega}$ coincides with the orbital angular velocity of the “star - planet” binary system. In such a rotating reference frame, the specific external force is determined by the expression

$$\mathbf{f} = -\nabla\Phi - 2(\boldsymbol{\Omega} \times \mathbf{v}). \quad (31)$$

Here the first term in the right-hand side describes the force due to the Roche potential gradient

$$\Phi = -\frac{GM_s}{|\mathbf{r} - \mathbf{r}_s|} - \frac{GM_p}{|\mathbf{r} - \mathbf{r}_p|} - \frac{1}{2}[\boldsymbol{\Omega} \times (\mathbf{r} - \mathbf{r}_c)]^2, \quad (32)$$

where M_s is the mass of the star, M_p — mass of the planet, \mathbf{r}_s — radius-vector of the stellar center, \mathbf{r}_p — radius-vector of the center of the planet, \mathbf{r}_c — radius-vector of the center of mass of the system. The second term describes the Coriolis force.

The background magnetic field was set as $\mathbf{H} = \mathbf{H}_p + \mathbf{H}_s$. The first term, \mathbf{H}_p describes the proper magnetic field of the planet. It was assumed in our model that hot Jupiters have a dipole magnetic field,

$$\mathbf{H}_p = \frac{\mu}{|\mathbf{r} - \mathbf{r}_p|^3} [3(\mathbf{d} \cdot \mathbf{n}_p)\mathbf{n}_p - \mathbf{d}], \quad (33)$$

where μ is magnetic momentum, $\mathbf{n}_p = (\mathbf{r} - \mathbf{r}_p)/|\mathbf{r} - \mathbf{r}_p|$, \mathbf{d} — unit vector, directed along magnetic axis, the vector of magnetic momentum $\boldsymbol{\mu} = \mu\mathbf{d}$. The second term, \mathbf{H}_s , describes the radial magnetic field of the stellar wind:

$$\mathbf{H}_s = \frac{B_0 R_s^2}{|\mathbf{r} - \mathbf{r}_s|^2} \mathbf{n}_s, \quad (34)$$

where R_s is stellar radius, while the vector $\mathbf{n}_s = (\mathbf{r} - \mathbf{r}_s)/|\mathbf{r} - \mathbf{r}_s|$. It is not difficult to ascertain that such a background magnetic field satisfies the potential condition $\nabla \times \mathbf{H} = 0$. Thus, in our model at the initial instant of time the proper magnetic field of the plasma \mathbf{b} will be defined by the azimuthal component of the magnetic field (19) only.

4.2 Numerical method

For the numerical solution of the equations of magnetic hydrodynamics, presented in the previous section, we use a combination of Roe [39] and Lax - Friedrichs [40, 41] difference schemes. Solution algorithm has several successive stages resulting from the application of splitting over physical processes. Suppose, we know the distribution of all quantities over computational grid at the time t^n . Then, to get the values at the next time instant $t^{n+1} = t^n + \Delta t$, let decompose the complete system of equations (26) - (29) into two subsystems.

The first subsystem corresponds to the ideal magnetohydrodynamics with proper magnetic field of the plasma \mathbf{b} without account for the background magnetic field \mathbf{H} :

$$\frac{\partial \rho}{\partial t} + \nabla \cdot (\rho \mathbf{v}) = 0, \quad (35)$$

$$\rho \left[\frac{\partial \mathbf{v}}{\partial t} + \mathbf{v} \cdot \nabla \mathbf{v} \right] = -\nabla P - \mathbf{b} \times \nabla \times \mathbf{b} - \rho \mathbf{f}, \quad (36)$$

$$\frac{\partial \mathbf{b}}{\partial t} = \nabla \times (\mathbf{v} \times \mathbf{b}), \quad (37)$$

$$\rho \left[\frac{\partial \varepsilon}{\partial t} + \mathbf{v} \cdot \nabla \varepsilon \right] + P \nabla \cdot \mathbf{v} = 0. \quad (38)$$

In our numerical model, to solve this system, the Roe scheme [42, 43] with Osher's incremental correction [44] (see also the monograph [35]) for magnetohydrodynamical equations was used. The magnetohydrodynamical version of the Roe scheme was introduced in the code in such a way that in the absence of a magnetic field ($\mathbf{b} = 0$) this scheme exactly transforms into Roe -infeldt - Osher scheme, which we used in purely gas-dynamical calculations [18].

The second subsystem accounts for the influence of the background field:

$$\rho \frac{\partial \mathbf{v}}{\partial t} = -\mathbf{H} \times \nabla \times \mathbf{b}, \quad (39)$$

$$\frac{\partial \mathbf{b}}{\partial t} = \nabla \times (\mathbf{v} \times \mathbf{H}). \quad (40)$$

The first equation in this subsystem describes the influence of the electromagnetic force, caused by the background field, while the second equation describes the generation of magnetic field. It is assumed that at this stage the density ρ and specific internal energy ε do not change. To solve the second subsystem, Lax-Friedrichs scheme with TVD (total variation diminishing) boost was applied [35]).

To clear the divergence of the magnetic field \mathbf{b} , we used the method of generalized Lagrange multiplier [45]. The choice of this method is due to the fact that the flow in the vicinity of the hot Jupiter is essentially unsteady, especially in the cocurrent stream, forming the magnetospheric tail.

5 Results of the modeling

As an example demonstrating the ideas presented in the paper, we computed the model of the flow structure in the vicinity of a hot Jupiter HD 209458b. It is the first transient hot Jupiter, discovered in 1999 [46]. The main parameters of the model corresponded to the values used in our previous studies (see, e.g., [18]). Parent star has spectral type G0, the mass $M_s = 1.15M_\odot$, the radius $R_s = 1.2R_\odot$. Proper stellar rotation is characterized by a period $P_{\text{rot}} = 14.4$ day, which corresponds to the angular velocity $\Omega_s = 5.05 \cdot 10^{-6} \text{ s}^{-1}$ or the linear velocity at the equator $v_{\text{rot}} = 4.2 \text{ km/s}$. The mass of the planet is $M_p = 0.71 M_{\text{jup}}$, its photometric radius $R_p = 1.38 R_{\text{jup}}$, where M_{jup} and R_{jup} are the mass and radius of the Jupiter, respectively. Semi-major axis of the planet orbit $A = 10.2R_\odot$, corresponding to the period of revolution $P_{\text{orb}} = 84.6 \text{ hr}$.

At the initial instant of time we set a spherically-symmetric isothermal atmosphere with density distribution defined by the following expression:

$$\rho = \rho_{\text{atm}} \exp \left[-\frac{GM_p}{R_{\text{gas}}T_{\text{atm}}} \left(\frac{1}{R_p} - \frac{1}{|\mathbf{r} - \mathbf{r}_p|} \right) \right], \quad (41)$$

where ρ_{atm} — the density at the photometric radius, T_{atm} — the temperature of the atmosphere, R_{gas} — gas constant.

The radius of the atmosphere was determined from the condition of pressure equilibrium with the matter of stellar wind. The following atmospheric parameters were used in the calculations: temperature $T_{\text{atm}} = 7500 \text{ K}$, the concentration of particles at photometric radius $n_{\text{atm}} = 10^{11} \text{ cm}^{-3}$.

As the parameters of the stellar wind, we used the corresponding parameters of the solar wind at the distance $10.2R_\odot$ from the center of the Sun [32]: temperature $T_w = 7.3 \cdot 10^5 \text{ K}$, velocity $v_w = 100 \text{ km/s}$, concentration $n_w = 10^4 \text{ cm}^{-3}$. Magnetic field of the wind was set by the formulas presented in the description of the numerical model.

Kislyakova et al. [47] have found from observational data that the magnetic moment μ of the hot Jupiter HD 209458b can not exceed the $0.1\mu_{\text{jup}}$, where $\mu_{\text{jup}} = 1.53 \cdot 10^{30} \text{ G} \cdot \text{cm}^3$ is the magnetic moment of Jupiter. The estimate of the magnetic moment of HD 209458b according to [48] is, approximately, $0.08\mu_{\text{jup}}$. In our calculations, we assumed that the magnetic moment of the hot Jupiter HD 209458b is $\mu = 0.1\mu_{\text{jup}}$. Magnetic axis of the dipole was tilted by the angle of 30° relative to the axis of rotation of the planet in the direction opposite to the star. At this, we considered that the proper rotation of the planet is synchronized with the orbital rotation and the axis of its own rotation is collinear with the axis of orbital rotation.

Computations were carried out in the Cartesian coordinate system, with the origin in the center of the planet. The x -axis connected the centers of the star and the planet and was directed from the star. The y -axis was directed along the orbital rotation of the planet, and the axis z — along its axis of proper rotation. The computational domain had dimensions $-30 \leq x/R_p \leq 30$, $-30 \leq y/R_p \leq 30$, $-15 \leq z/R_p \leq 15$, the number of cells was $N = 480 \times 480 \times 240$. To increase the spatial resolution in the atmosphere of the planet, we used the grid, exponentially condensing to the center of the planet. Characteristic size of the cell at the photometric radius of the planet was $0.02R_p$, while at the outer edge of the computational domain the cell size was equal, approximately, to $0.4R_p$. The boundary conditions were the same as in our recent work [24].

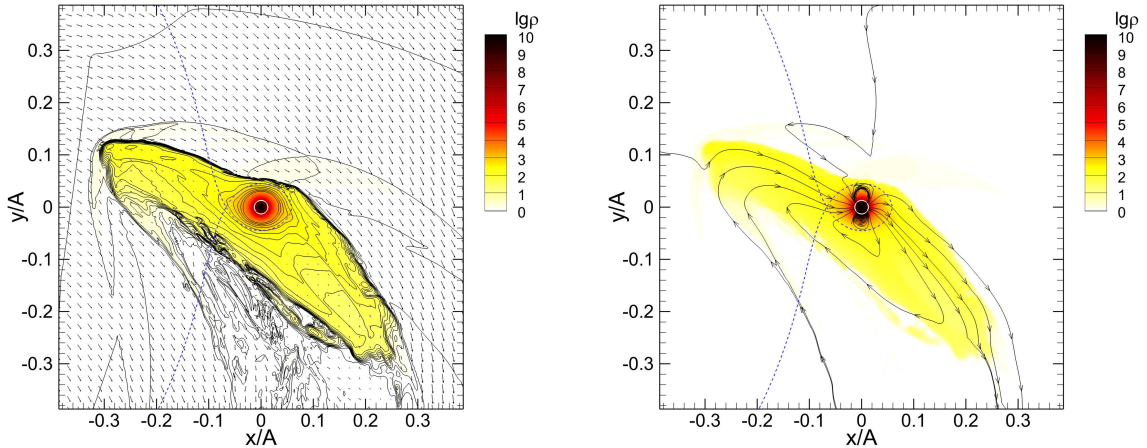


Fig. 9. Distribution of density (color scale and contours), velocity (the arrows, left panel), and magnetic field (the lines with arrows, right panel) in the orbital plane of the hot Jupiter for the case of a weak magnetic field of the wind (model 1). Solution is presented for the time $0.23P_{\text{orb}}$ from the beginning of computations. The dashed line shows the boundary of the Roche lobe. Light circle corresponds to the photometric radius of the planet. (Color version of the Figure is available in the electronic version of the journal.)

We carried out two calculations, which differed only in the value of the parameter B_0 , which determines the average magnetic field at the surface of the star. In the first run (model 1), B_0 was set to 10^{-4} G. This corresponds to a weak magnetic field of the stellar wind. In the second run (model 2), $B_0 = 1$ G was used (strong field). This corresponds to the average magnetic field of the quiet Sun. Results of calculations are presented in Figs. 9 and 10. The Figures show density distribution (by gradations of color and contours), velocity (the arrows in the panels to the left), and magnetic field (the lines with the arrows in the panels to the right) in the orbital plane of a hot Jupiter. The density is normalized to the wind density at the orbit of the planet ρ_w . Presented numerical solutions correspond to the time $0.23P_{\text{orb}}$ from the start of the computations. The border of the Roche lobe is shown by a dotted line. The planet is located in the center of the computational domain and is depicted by a light circle, the radius of which corresponds to the photometric radius.

In both models two powerful streams form from the neighborhood of the Lagrange points L_1 and L_2 . The first stream is formed on the day side, it is directed toward the star and, therefore, it moves against the wind under the influence of its gravity. The second stream begins on the night side and forms a wide turbulent plume behind the planet.

In model 1, as a result of the interaction of the stellar wind with the envelope of the planet, a detached shock wave forms, well visible in Fig. 9. One can say that it consists of two separate shock waves, one of which arises around the atmosphere of the planet, while the other — around the jet from the inner Lagrange point L_1 . In the right panel of Fig. 9 it is seen that inside Roche lobe of the planet magnetic field remains close to the dipole. However, in the outflows magnetic field lines are drawn by plasma flows.

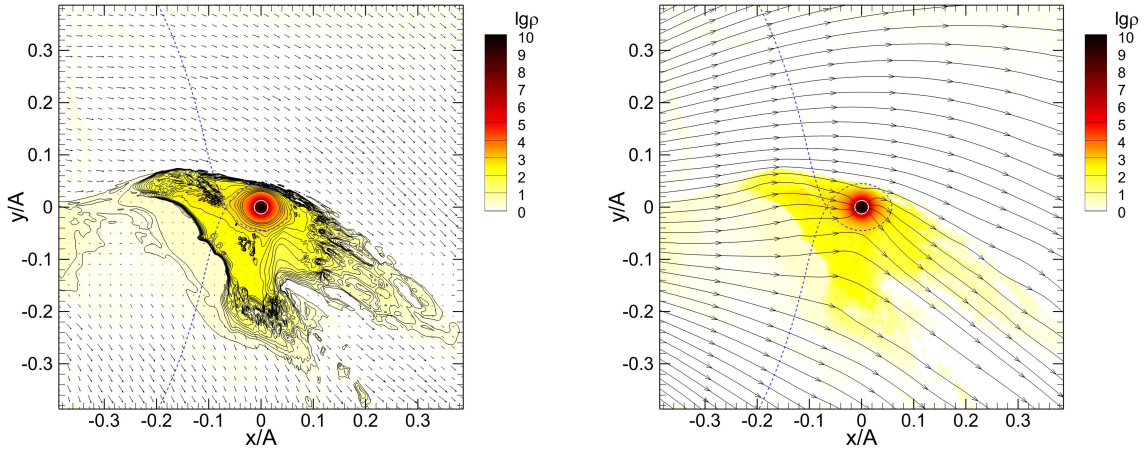


Fig. 10. Same as in Fig. 9, but for the model 2.

Magnetic field of the stellar wind in this model is so weak that it plays no dynamic role. In fact, it manifests itself as a kind of a passive impurity present in the wind plasma. Such a magnetosphere obviously corresponds to the *A1* subtype in the case of an open ionospheric envelope of the hot Jupiter, the structure of which is schematically shown in the right panel of Fig. 5.

In the model 2, the interaction of the stellar wind with the envelope of the planet is shock-less. In the left panel of Fig. 10 it is seen that detached shock does not form neither around the atmosphere of the planet nor around the jet from the point L_1 . Strong magnetic field of the wind impedes free motion of the matter in the direction transverse to the lines of force. Therefore, the flow pattern in this model differs significantly from that in the model 1, because in this case, apart of stellar gravity, the centrifugal force, and Coriolis force, an essential role also belongs to the electromagnetic force, due to the magnetic field of the wind. The tail by the planet is also oriented at a different angle, since the flows in it are aligned mainly along the magnetic field lines. Magnetic field of the wind is slightly distorted by the streams from the planet (see the right panel in Fig. 10), but, generally, retains its original structure. The magnetosphere in model 2 corresponds to the *B2* subtype in the case of open ionospheric envelope of the hot Jupiter; its structure is shown schematically in the right panel of Fig. 8.

Comparison of results of computations for two models, allows to make the following conclusions. Magnetic field of the stellar wind is an important factor, affecting the process of the outflow of the ionospheric envelope from the Roche lobe of a hot Jupiter. In the case of a weak wind field, the main limiting factor is dynamic wind pressure. As the field increases, the total wind pressure increases. As a result, for the same other parameters, the dimensions of the quasi-closed ionospheric envelope decrease. In the model 2 in the direction of the star (x -axis) the size of the envelope turned out to be by a factor 1.5 smaller compared to the case of weak field (model 1). In model 1, in the direction of the orbital motion of the planet (y - axis) the envelope moves away from the planet to the distance of about 10 photometric radii, whereas in model 2 this distance is approximately 5 photometric radii. Note, just these characteristics of the envelope

(in the direction of the orbital motion of the planet) determine the observed phenomena during the transit, associated with the early onset of the eclipse in the near ultraviolet range [7]. Consequently, the observed properties of the early onset of eclipse during the transit are also dependent on the strength of the wind magnetic field.

6 Conclusion

The analysis performed in this paper leads to the conclusion that many hot Jupiters may be located in the sub-Alfvén zone of the stellar wind of the parent star. This means that in the studies of the flow of the stellar wind around the atmosphere of a hot Jupiter magnetic field of the wind is an extremely important factor, consideration of which is absolutely necessary, both in theoretical models and in the interpretation of observational data. The fact is that in the sub-Alfvén zone magnetic pressure of the stellar wind exceeds its dynamic pressure even if the orbital motion of the planet is taken into account.

Based of rather simple model considerations, as well as summarizing the results of numerical experiments, we suggested a classification of possible shapes of magnetospheres of hot Jupiters. In particular, well studied magnetospheres of the Earth and Jupiter in our classification belong to the subtype *A1* (intrinsic magnetosphere with bow shock) with closed envelopes. As it was shown by the analysis of observational data, the magnetospheres of many hot Jupiters can belong to the subtype *B2* (shock less induced magnetosphere). In this case, magnetic field of the wind is rather strong and, therefore, the flow of the stellar wind around the atmosphere of the planet appears to be shock-less. Detached shock waves around the atmosphere and the outflow from the Lagrange point L_1 do not form. The structure of such a magnetosphere is fundamentally different from the magnetosphere of terrestrial type.

However, since the characteristics of the stellar wind can vary quite a bit over time (approximately, by a factor 1.5 to 2), a fraction of hot Jupiters falls into the parameter space, which we figuratively named “gray area”. In this zone, the type of stellar wind flow around the planet is intermediate between a shock and a shock-less flow. The study of the structure of the magnetospheres of this type is a separate task.

To study the process of the flow of stellar wind around hot Jupiters with simultaneous consideration of both the planet magnetic field and the wind magnetic field, we developed a relevant three-dimensional magnetohydrodynamical numerical model. The basis of our numerical model is Roe-Einfeldt-Osher difference scheme of higher order approximation for the equation of ideal magnetohydrodynamics. In our numerical model, the total magnetic field is represented as a superposition of the external magnetic field and the magnetic field induced by electric currents in the plasma itself. As an external field we applied superposition of the dipole magnetic field of the planet and the radial component of the wind magnetic field. In the numerical algorithm, the factors associated with the presence of the external magnetic field were taken into account at a separate step using appropriate difference scheme of Godunov type.

We calculated two models that differ by the strength of the average magnetic field at the surface of the star only. In the first model the wind magnetic field was weak and the flow pattern matched well both purely gas-dynamical calculations [18] and calculations

taking into account the magnetic field of the planet only [24]. These models give a similar picture of the supersonic flow around the planet, since the proper magnetic field of a hot Jupiter is quite weak. In the terms of our classification, the corresponding magnetosphere belongs to the *A1* subtype (intrinsic magnetosphere with bow shock) with an open ionospheric envelope. For such parameters the planet is in the super-Alfvén zone of the wind and in its interaction with the wind a detached shock wave is formed. In the second model, the magnetic field of stellar wind corresponded to the magnetic field of the solar wind, which is defined by the average magnetic field of the quiet Sun. In this case, the hot Jupiter falls into the sub-Alfvén wind zone and, therefore, the detached shock wave does not form, just as it observed in the calculations. In terms of our classification, such a magnetosphere belongs to the subtype *B2* (shockless induced magnetosphere) with an open ionospheric envelope.

Acknowledgements

The authors acknowledge P.V. Kaigorodov for useful discussions. This study was supported by RSF (project 18-12-00447). Computations were carried out using the supercomputer of the National Research Center “Kurchatov Institute”.

References

- [1] E.S. Belenkaya, *Phys. Usp.* **52**, 7658 (2009).
- [2] M. Sounders, in *Advances in solar system magnetohydrodynamics*, p. 357, (eds. E.R. Priest, A.W. Hood) (Cambridge University Press, Cambridge, 1991).
- [3] R.A. Murray-Clay, E.I. Chiang, N. Murray, *Astrophys. J.* **693**, 23 (2009).
- [4] M. Mayor, D. Queloz, *Nature* **378**, 355 (1995).
- [5] D. Lai, C. Helling, E.P.J. van den Heuvel, *Astrophys. J.* **721**, 923 (2010).
- [6] S.-L. Li, N. Miller, D.N.C. Lin, J.J. Fortney, *Nature* **463**, 1054 (2010).
- [7] A. Vidal-Madjar, A. Lecavelier des Etangs, J.-M. Desert, G.E. Ballester, et al., *Nature* **422**, 143 (2003).
- [8] A. Vidal-Madjar, A. Lecavelier des Etangs, J.-M. Desert, G.E. Ballester, et al., *Astrophys. J.* **676**, L57 (2008).
- [9] L. Ben-Jaffel, *Astrophys. J.* **671**, L61 (2007).
- [10] A. Vidal-Madjar, J.-M. Desert, A. Lecavelier des Etangs, G. Hebrard, et al., *Astrophys. J.* **604**, L69 (2004).
- [11] L. Ben-Jaffel, S. Sona Hosseini, *Astrophys. J.* **709**, 1284 (2010).
- [12] J.L. Linsky, H. Yang, K. France, C.S. Froning, et al., *Astrophys. J.* **717**, 1291 (2010).

- [13] R.V. Yelle, *Icarus* **170**, 167 (2004).
- [14] A. Garcia Munoz, *Planet. Space Sci.* **55**, 1426 (2007).
- [15] T.T. Koskinen, M.J. Harris, R.V. Yelle, P. Lavvas, *Icarus* **226**, 1678 (2013).
- [16] D.E. Ionov, V.I. Shematovich, Ya.N. Pavlyuchenkov, *Astron. Rep.* **61**, 387 (2017).
- [17] D. Bisikalo, P. Kaygorodov, D. Ionov, V. Shematovich, et al., *Astrophys. J.* **764**, 19 (2013).
- [18] D.V. Bisikalo, P.V. Kaigorodov, D.E. Ionov, V.I. Shematovich, *Astron. Rep.* **57**, 715 (2013).
- [19] A.A. Cherenkov, D.V. Bisikalo, P.V. Kaigorodov, *Astron. Rep.* **58**, 679 (2014).
- [20] D.V. Bisikalo, A.A. Cherenkov, *Astron. Rep.* **60**, 183 (2016).
- [21] A.A. Cherenkov, D.V. Bisikalo, L. Fossati, C. Mostl, *Astrophys. J.* **846**, 31 (2017).
- [22] A.A. Cherenkov, D.V. Bisikalo, A.G. Kosovichev, *Mon. Not. R. Astron. Soc.* **475**, 605 (2018).
- [23] D.V. Bisikalo, V.I. Shematovich, A.A. Cherenkov, L. Fossati, C. Mostl, *Astrophys. J.* **869**, 108 (2018).
- [24] A.S. Arakcheev, A.G. Zhilkin, P.V. Kaigorodov, D.V. Bisikalo, A.G. Kosovichev, *Astron. Rep.* **61**, 932 (2017).
- [25] D.V. Bisikalo, A.S. Arakcheev, P.V. Kaigorodov, *Astron. Rep.* **61**, 925 (2017).
- [26] W.-H. Ip, A. Kopp, J.H. Hu, *Astrophys. J.* **602**, L53 (2004).
- [27] D. Fabbian, R. Simoniello, R. Collet, et al., *Astron. Nachr.* **338**, 753 (2017).
- [28] H. Lammer, M. Gudel, Y. Kulikov, et al., *Earth Planets Space*, **64**, 179 (2012).
- [29] M.J. Owens, R.J. Forsyth, *Living Rev. Solar Phys.* **10**, 5 (2013).
- [30] E.N. Parker, *Astrophys. J.* **128**, 664 (1958).
- [31] V.B. Baranov, R.B. Krasnobaev, *Hydrodynamical theory of space plasma* (Nauka, Moscow, 1977) [in Russian].
- [32] G.L. Withbroe, *Astrophys. J.* **325**, 442 (1988).
- [33] C.T. Russell, *Rep. Prog. Phys.* **56**, 687 (1993).
- [34] L.D. Landau, E.M. Livshitz, *Electrodynamics of Continuous Media* (Nauka, Moscow, 1982; Pergamon, New York, 1984).
- [35] D.V. Bisikalo, A.G. Zhilkin, A.A. Boyarchuk, *Gas Dynamics of Close Binary Stars* (Fizmatlit, Moscow, 2013) [in Russian].

- [36] A.G. Zhilkin, D.V. Bisikalo, A.A. Boyarchuk, *Phys. Usp.* **55**, 115 (2012).
- [37] T. Tanaka, *J. Comp. Phys.* **111**, 381 (1994).
- [38] K.G. Powell, P.L. Roe, T.J. Linde, T.I. Gombosi, D.L. de Zeeuw, *J. Comp. Phys.* **154**, 284 (1999).
- [39] P.L. Roe P.L., *Lect. Notes Phys.* **141**, 354 (1980).
- [40] P.D. Lax, *Commun. Pure Appl. Math.* **7**, 159 (1954).
- [41] R.O. Friedrichs R.O., *Commun. Pure Appl. Math.* **7**, 345 (1954).
- [42] P. Cargo, G. Gallice, *J. Comp. Phys.* **136**, 446 (1997).
- [43] A.G. Kulikovskii, N.V. Pogorelov, A.Yu. Semenov, *Mathematical Aspects of Numerical Solution of Hyperbolic Systems* (Fizmatlit, Moscow, 2001; Chapman and Hall/CRC, Boca Raton, 2000).
- [44] S.R. Chakravarthy, S. Osher, AIAA Papers N 85-0363 (1985).
- [45] A. Dedner, F. Kemm, D. Kroner, C.-D. Munz, T. Schnitzer, M. Wesenberg, *J. Comp. Phys.* **175**, 645 (2002).
- [46] D. Charbonneau, T.M. Brown, D.W. Latham, M. Mayor, *Astrophys. J.* **529**, L45 (2000).
- [47] K.G. Kislyakova, M. Holmström, H. Lammer, et al., *Science.* **346**, 981 (2014).
- [48] D.J. Stevenson, *Reports on Progress in Physics.* **46**, 555 (1983).